

In Situ ESR/UV–vis–NIR and ATR-FTIR Spectroelectrochemical Studies on the p-Doping of Copolymers of 3-Methylthiophene and 3-Hexylthiophene

Luis F. Cházaro-Ruiz,[†] Andrea Kellenberger,^{‡,§} and Lothar Dunsch^{*,†}

Abteilung Elektrochemie und Leitfähige Polymere, Leibniz-Institut für Festkörper- und Werkstofforschung, Helmholtzstrasse 20, D-01069 Dresden, Germany, and Faculty of Industrial Chemistry and Environmental Engineering, University “Politehnica” of Timisoara, Piata Victoriei 2, RO-300006 Timisoara, Romania

Received: July 31, 2008; Revised Manuscript Received: December 22, 2008

A combined spectroelectrochemical study by ESR/UV–vis–NIR as well as FTIR spectroscopy on the influence of the copolymer composition on the stabilization of charges upon electrochemical p-doping is presented. As compared to the parent homopolymers 3-hexylthiophene (**3-HeTh**) and 3-methylthiophene (**3-MeTh**) which seems to be irregular, FTIR studies of the copolymer of both monomers (**copMeHeTh**) point to a regioregular structure. The *in situ* ESR and UV–vis–NIR spectroelectrochemistry at higher doping levels of the polymeric materials proves bipolarons and polaron pairs as stable charged states in poly(3-hexylthiophene) as well as the copolymer **copMeHeTh**. During the p-doping of poly(3-methylthiophene) bipolarons are the dominating species at higher doping levels. It is demonstrated that only the simultaneous use of both the ESR and the UV–vis–NIR spectroscopy enables the differentiation of polarons (paramagnetic) and polaron pairs (diamagnetic) in a conducting polymer.

Introduction

Conjugated polymers, such as poly(3-alkylthiophenes) (**PAThs**), have been extensively studied owing to their high stability of both their doped and undoped states as well as their structural versatility. The variation of the monomer structure by alkyl-side modification results in a broad modulation of the polymer morphology as well as electronic and electrochemical properties of the conjugated polymers. All these properties have led to significant developments in applications such as electric conductors, electrode materials, organic semiconductors, sensors, electrochromic devices, and transistors.¹ Moreover, polythiophenes have been often considered as a model for the study of charge transport in conducting polymers with a degenerate or nondegenerate ground state.²

Among the poly(3-alkylthiophene) precursors are 3-methylthiophene (**3-MeTh**) and 3-hexylthiophene (**3-HeTh**) monomers which are very useful in copolymerization reactions as starting materials together with other thiophene derivatives. The copolymerization reaction of two monomer units is used to combine desirable properties of two polymers like desired electrochromic properties and high electrical conductivities. It has been recognized that the copolymerization of 3-alkylthiophene derivatives leads to a higher thermal stability of doped **PAThs**³ which is a tremendous problem for their application.⁴ To achieve this aim, random copolymers of **3-MeTh** and 3-octylthiophene have been prepared.³ The thermal undoping is significantly suppressed, and this effect has been attributed to the statistical decrease of the side-chain interactions. The effect of the copolymerization between **3-MeTh** and **3-HeTh** has also been discussed in terms of a new material which still has excellent solubility together with high electrical conductivity, even higher than the conductivity of poly(3-hexylthiophene).⁵ This observation is attributed to the presence of **3-MeTh**

moieties since this monomer shows an exceedingly high conductivity among the polythiophenes.⁶ It was also found that the resultant copolymer has a good stretchability.

In this contribution an *in situ* ESR UV–vis–NIR and a FTIR spectroelectrochemical study of the copolymer (**copMeHeTh**) from 3-methylthiophene and 3-hexylthiophene on ITO electrodes is performed. The use of several *in situ* spectroelectrochemical techniques results in the direct detection of both the paramagnetic and diamagnetic species formed during electrochemical doping of such a copolymer. The structure of the copolymer is studied by *in situ* FTIR spectroelectrochemistry. This study is devoted to the description of the influence of the random distribution of the long side alkyl chain of the **3-HeTh** in the formation and stability of the charge carriers during the p-doping of the copolymer **copMeHeTh** using *in situ* ESR/UV–vis spectroelectrochemistry. These results are compared with those from the spectroelectrochemical study of the p-doping of the corresponding homopolymers poly(3-methylthiophene) (**p-3-MeTh**) and poly(3-hexylthiophene) (**p-3-HeTh**). To the best of our knowledge, there are no reports concerning the *in situ* ESR/UV–vis–NIR spectroelectrochemical study of the charge carriers involved in the mechanism of the electrochemical oxidation of the copolymer from **3-MeTh** and **3-HeTh**. The simultaneous use of ESR and optical spectroscopies does allow us to differentiate the nature of the charge carriers electrogenerated during the p-doping and to get the individual spectra of each intermediate.

Experimental Section

Chemicals. Acetonitrile (ACN, puriss., absolute, $\geq 99.5\%$ GC, $w(\text{H}_2\text{O}) \leq 0.001\%$) purchased from Fluka and ferrocene (p.a., $\geq 98\%$) from Merck were used as received. Acetonitrile was stored over molecular sieves. Tetrabutylammonium hexafluorophosphate (*n*-Bu₄NPF₆, puriss., electrochemical grade, $\geq 99.0\%$ CHN) from Fluka was dried under reduced pressure at 80 °C for 24 h before use. All solutions were deaerated with nitrogen

* To whom correspondence should be addressed.

[†] Leibniz-Institut für Festkörper- und Werkstofforschung.

[‡] University “Politehnica” of Timisoara.

prior to the measurements for 10 min, and during the measurements the solutions were passed over by a stream of nitrogen.

Spectroscopic Measurements. In situ ESR/UV-vis-NIR spectroelectrochemical experiments were performed in the flat ESR cell filled with solutions of acetonitrile + 0.1 M of *n*-Bu₄NPF₆ as supporting electrolyte. A platinum wire served as a counter electrode and a silver wire coated with AgCl as a pseudoreference electrode. The potentials, referred to ferrocene-ferrocenium (Fc/Fc⁺) redox couple (0.353 V vs Ag/AgCl), were estimated using ferrocene as an internal standard added after the measurements. As a working electrode a laminated indium tin oxide (ITO) glass layer was used. The detailed preparation of laminated electrodes was reported elsewhere.⁷ The spectroelectrochemical experiments were done in the optical ESR cavity OR280 (Bruker, Karlsruhe, Germany) using an ELEXYS X-band spectrometer (Bruker, Germany) or an EMX X-band spectrometer (Bruker, Germany). As a diode array UV-vis-NIR spectrometer the system TIDAS (J&M, Aalen, Germany) was used. A halogen lamp served as a light source and was connected via optical wave guides to the optical ESR cavity like the diode array spectrometer. Both the ESR spectrometer and the UV-vis-NIR spectrometer were linked to a PG 285 potentiostat (HEKA-Elektronik Lambrecht, Germany). The triggering was done by the software package PotPulse. The spectra were recorded at constant electrode potentials changed by steps within the same equidistant intervals which divide the cyclic voltammogram. During one cyclic voltammogram 23, 27, and 25 ESR/UV-vis-NIR spectra were recorded for the **p-3-MeTh**, **p-3-HeTh**, and **copMeHeTh** films, respectively. Only relative intensities of the ESR and UV-vis-NIR spectra have been calculated because the thickness of the films is unknown. However, it has been observed^{7a} that the well-defined ESR/UV-vis-NIR spectra as well as cyclic voltammograms in the scan range 5–100 mV s⁻¹ reflect the homogeneity and quality of the polymer films prepared for this study.

Ex situ and *in situ* FTIR measurements were performed with the attenuated total reflection (ATR) technique, using an IFS 66v spectrometer (Bruker, Germany) with a DTGS detector working at room temperature. *Ex situ* FTIR spectra were recorded for **p-3-MeTh**, **p-3-HeTh**, and **copMeHeTh** films prepared in a conventional electrochemical cell, according to the method described below. After the deposition on ITO layer electrodes, the polymer films were carefully peeled off and transferred to the ZnSe internal reflection element. For the *in situ* FTIR measurements a self-designed spectroelectrochemical cell was used. Details of the construction of the cell are given elsewhere.⁸ Since ZnSe is a nonconductive material, it has to be covered by a conductive layer of gold for the *in situ* spectroelectrochemical measurements. In our study a fine gold grid with a thickness of 50 nm was deposited on the ZnSe crystal. The gold grid consists of a complex geometry with stripes having a thickness of 7.5 and 9.3 μm with a distance of 4.3 and 6.7 μm between the stripes and 37.3 and 47.1 μm, respectively, between the patterns. To improve the adherence of the gold film, an intermediate adhesive Cr layer with a thickness of 5 nm was used. Polymer films were prepared on the ZnSe-Au working electrode from a solution containing 0.02 M **3-MeTh** and 0.04 M **3-HeTh** by the pulse deposition technique. The electrode potential was increased from an initial value of -0.43 V, where no faradaic current was observed up to 1.37 V, and then lowered and maintained constant at 1.27 V to avoid the overoxidation of the copolymer film. *In situ* FTIR spectra at several equidistant time intervals were taken during the electropolymerization in order to characterize the resultant

material. The p-doping behavior of the prepared polymer films was studied by cyclic voltammetry using a HEKA PG 287 potentiostat. The voltammograms were recorded at low scan rates (5 mV s⁻¹) in a 0.1 M *n*-Bu₄NPF₆ acetonitrile solution purged for 20 min with nitrogen prior to the determinations. Simultaneously with the cyclic voltammograms *in situ* FTIR spectra were taken. For each spectrum 50 interferograms were accumulated with a resolution of 4 cm⁻¹, covering a range of about 150 mV in the cyclic voltammogram. A spectrum recorded before the electrochemical experiment was used as a reference spectrum.

Films Preparation for the *in Situ* ESR/UV-vis-NIR Spectroelectrochemical Experiments. The films of **p-3-MeTh**, **p-3-HeTh**, and **copMeHeTh** on a transparent laminated ITO electrode were prepared electrochemically in a conventional three-electrode cell containing acetonitrile solution and 0.1 M *n*-Bu₄NPF₆ as supporting electrolyte. A platinum wire served as a counter electrode and a silver wire coated with AgCl as the pseudoreference electrode. The potentials, referred to ferrocene-ferrocenium (Fc/Fc⁺) redox couple (0.353 V vs Ag/AgCl), were estimated using ferrocene as an internal standard added after the measurements. The concentration of monomer in solution was 0.02 M for **3-MeTh** and 0.04 M for **3-HeTh**. A mixture of **3-MeTh:3-HeTh** with a molar ratio 1:2 was used in the polymerization of the copolymer. The films were electropolymerized on the laminated ITO electrode by application of a pulse potential at 1.147 V (**3-MeTh**), 1.347 V (**3-HeTh**), and 1.347 V (**3-MeTh:3-HeTh**). Before the application of these pulses, the potential was increased from a value where no redox reaction occurs (-0.353 V) up to the value of the constant pulse for the electropolymerization. The reference electrode was separated from the solution via a junction containing supporting electrolyte. The polymer films were washed with pure acetonitrile in order to remove the unreacted monomers and then dried at room temperature. After polymerization the working electrode was transferred to the flat cell used for the ESR/UV-vis-NIR experiments and kept under a nitrogen atmosphere. The color of the dedoped films was deep blue (**p-3-MeTh**), red-brown (**p-3-HeTh**), and dark red-brown for the copolymer **copMeHeTh**.

Results and Discussion

Electrochemical Synthesis of the Copolymer. It was mentioned that the copolymerization of two (or more) thiophene monomers is important for attempts to achieve a high conductivity compatible with good processability. It has been reported that the copolymerization reaction was performed with the **3-MeTh:3-HeTh** ratio of 1:2 by an organosynthetic method, and a copolymer with high conductivity and good stretchability was obtained.⁵ In this study the electrochemical synthesis of the copolymer was performed with a reaction system where the **3-MeTh:3-HeTh** ratio was the same: 1:2. The conditions for the electrocopolymerization take into account that the electrochemical oxidation of **3-MeTh** occurs at lower potential than the **3-HeTh**.⁵ This implies that a sample of our copolymer has a mixture of both monomers.

FTIR Characterization of the Polymer Films. The film preparation technique is important because it determines the degree of order of the polymers in terms of regioregularity which denotes the percentage of stereoregular head-to-tail (HT) attachments of the alkyl side chains to the 3-position of the thiophene rings, one of the most important characteristics of poly(3-alkylthiophenes). It has been reported that the *in situ* FTIR studies can give information on the degree of regioregu-

TABLE 1: Characteristic IR Bands and Their Structural Assignments

polymer	aromatic C–H stretch	aliphatic C–H stretch	ring stretch	–CH ₃ def	aromatic C–H out-of-plane	–CH ₃ rock
p-3-MeTh	3059	2957, 2918, 2849	1503, 1468	1388	827	
p-3-HeTh	3053	2951, 2918, 2850	1510, 1456	1372	829	723
copMeHeTh	3053	2950, 2918, 2850	1510, 1456	1388	822	716

larity of polymer chains in **PATHs**.^{9–11} Side chains of adjacent rings in **PATHs** can be in head-to-tail (HT) or in head-to-head (HH) conformation, resulting in four triad regioisomers: HT–HT, HT–HH, TT–HT, and TT–HH triad. **PATHs** with only HT–HT triad (regioregular **PATHs**) lead to a minimal steric hindrance and an extended π -conjugation length as a result of self-organization of **PATHs** main chains, whereas the HH or TT junctions result in spatially disordered polymer chains with limited conjugated segments.^{2b} The regioregular **PATHs** forms larger and better ordered regions than less regioregular. The regioregularity has practical importance in designing **PATHs**-based light-emitting diodes,¹² for example, some regioregular **PATHs** like **p-3-HeTh**, poly(3-octylthiophene), and poly(3-decylthiophene) present high luminescence.¹³ The degree of self-ordering and orientation of the stacks is also known to depend greatly on the film preparation technique.¹⁴

The **p-3-MeTh**, **p-3-HeTh**, and **copMeHeTh** films synthesized in the conventional electrochemical cell were characterized by FTIR spectroscopy. The main vibrations observed in the spectra together with their assignments are given in Table 1.

For the qualitative analysis of the FTIR spectra of substituted polyalkylthiophenes two criteria have been proposed, namely the position of the aromatic C–H out-of-plane vibration^{9,11} and the intensity ratio of the symmetric and antisymmetric ring stretch modes.¹⁰ According to the first criterion, the band position of the aromatic C–H out-of-plane vibration is shifted to lower wavenumbers for regioregular **PATHs** (820–822 cm^{−1}) and to higher wavenumbers for regiorandom **PATHs** (827–829 cm^{−1}). For **p-3-MeTh** and **p-3-HeTh** this band is situated at 827 and 829 cm^{−1}, respectively, which points to a random structure. For **copMeHeTh** the same band appears at 822 cm^{−1}, indicating a more ordered polymer chain. A measure of the conjugation length in the polymer backbone is given by the ratio $I_{\text{sym}}/I_{\text{asym}}$, lower ratios being associated with longer conjugated segments. The calculated ratios are 4.8 for **p-3-HeTh** and about half of this value for **p-3-MeTh** (2.6) and **copMeHeTh** (2.2). These results are consistent with a higher conjugation length of the copolymer in accordance with its regioregular structure. In contrast, the FTIR data suggest that the parent homopolymers **p-3-HeTh** and **p-3-MeTh** have a regiorandom structure.

Cyclic Voltammetry. Cyclic voltammograms of thin films of poly(3-methylthiophene) (**p-3-MeTh**), poly(3-hexylthiophene) (**p-3-HeTh**), and the copolymer **copMeHeTh** on ITO electrodes are given in Figure 1. The cyclic voltammetry was done in monomer-free solutions of acetonitrile with 0.1 M *n*-Bu₄NPF₆ as supporting electrolyte. All the scans started at −0.53 V toward anodic direction and were performed at a scan rate of 5 mV s^{−1}. The **p-3-MeTh** film (Figure 1C) exhibits a sharp anodic peak at 0.27 V and two cathodic peaks: a broad one at 0.31 V and a sharp peak at −0.2 V. The **p-3-HeTh** film (Figure 1B) shows two broad anodic peaks at 0.47 and 0.71 V and a cathodic broad peak at 0.21 V. The copolymer **copMeHeTh** film (Figure 1A) presents a broad anodic peak at higher potentials (0.48 V) than the first broad peak from **p-3-HeTh**, and also the corresponding broad cathodic peak is found at a higher potential of 0.27 V. In contrast to **p-3-MeTh**, a second cathodic peak at a more positive potential, −0.05 V, is detected. It has been reported that the cyclic voltammetry response of

p-3-HeTh is a function of the degree of regioregularity. The films with 70% and 81% of regioregularity present two anodic waves and one broad cathodic peak,¹⁵ while a film with 97% exhibits three pairs of redox peaks. Our voltammetric results might suggest that the **p-3-HeTh** film on ITO has a regioregularity within the range 70–81%. When the regioregularity is about 54%, no prepeak is observed. It has been suggested that the consecutive peaks of the voltammogram reflects different kinds of segments with a certain type of morphology, crystallinity, and conjugation lengths.¹⁶ The decrease in peak height and the positive shift of the prepeaks with the decrease in regioregularity may be explained by the decrease in both the amount and extension of the crystalline region. However, the cyclic voltammetry features of the **p-3-HeTh** in this work resemble those of a cast film of poly(3-hexylthiophene) with a regioregularity of ~54% which is less ordered and conjugated (regiorandom structure) and also appears to be yellow-brown as already reported elsewhere.¹⁷ The regiorandom structure of the **p-3-HeTh** film is also in agreement with the FTIR data, but from these data and the voltammetric features it is not possible to estimate the degree of regioregularity.

In situ ATR-FTIR spectra were taken during the copolymerization by the potential pulse method. The spectra obtained for **copMeHeTh** film growth from a solution containing both monomers **3-MeTh** (0.02 M) and **3-HeTh** (0.04 M) are given in Figure 2 for the wavenumber region 1600–700 cm^{−1}. The spectra sequence starts from the bottom of Figure 2, and several spectra are presented for different polymerization times. A spectrum taken before the start of the electrochemical polymerization for the cell containing the monomers solution was used as a reference spectrum. Thus, only changes induced by the polymer film deposition on the surface of the electrode can be

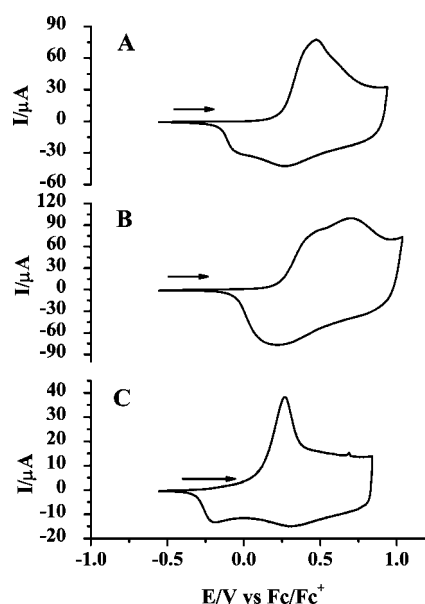


Figure 1. Cyclic voltammetry of **copMeHeTh** (A), **p-3-HeTh** (B), and **p-3-MeTh** (C) films on ITO electrode (diameter 3 mm) in acetonitrile + 0.1 M *n*-Bu₄NPF₆ at a scan rate of 0.005 V s^{−1}. All scans started at −0.53 V/Fc⁺/Fc toward the anodic direction.

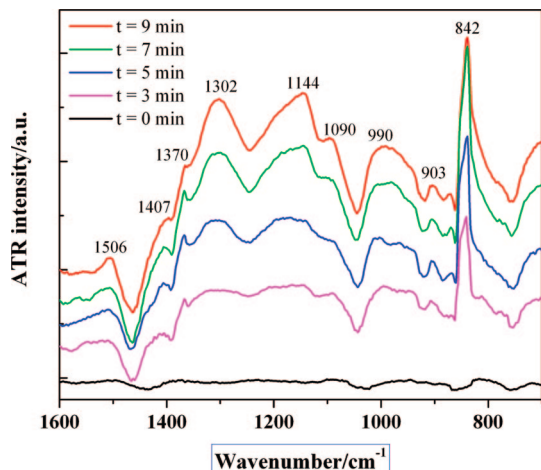


Figure 2. *In situ* ATR-FTIR spectra during the pulse potential copolymerization of 0.02 M **3-MeTh** and 0.04 M **3-HeTh** taken at equidistant time intervals. The applied potential varied from -0.43 to 1.37 V and then was kept constant at 1.27 V.

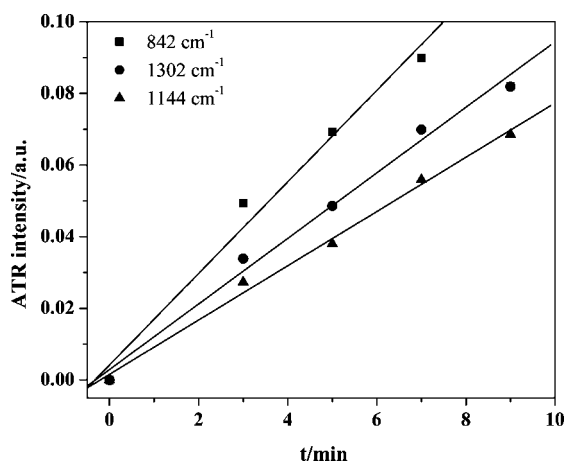


Figure 3. Dependence of the relative ATR intensity of doping-induced bands versus polymerization time for **copMeHeTh**.

seen. The first changes appear from the second spectra in Figure 2 and are dominated by some broad absorption bands which develops in three absorption peaks centered at 1302, 1144, and 990 cm^{-1} with bandwidth larger than 100 cm^{-1} . These doping induced bands appear during the chemical, electrochemical, or photoinduced doping of polyalkylthiophenes. The position of these bands does not depend on the type of doping or on the nature of the dopant anion. The literature data indicate that the doping induced bands appear around 1330, 1200, 1120, and 1020 cm^{-1} for polythiophene¹⁸ and at 1308, 1203, 1165, and 976 cm^{-1} for poly(3-methylthiophene). Also, a sharp peak is observed at 842 cm^{-1} ascribed to the PF_6^- anions incorporated into the copolymer film to compensate the positive charge created during the oxidative polymerization. The relative intensity of these vibrations increases linearly with the polymerization time as given in Figure 3. Besides the doping-induced bands, the *in situ* spectra in Figure 2 show additional bands attributed to the formed copolymer film. Vibrations at 1506 and 1407 cm^{-1} originate from the thiophene ring stretching and vibrations at 1370 and 990 cm^{-1} are assigned to the side alkyl chain.^{19,20}

In situ ATR-FTIR measurements during the p-doping of the copolymer film (here not shown) were carried out during cyclic voltammetric scan. The profile of the FTIR spectra shows a typical behavior for substituted **PATHs**, characterized by the

development of two distinct vibrational patterns: the range 1600–700 cm^{-1} where some very intense infrared-active vibration (IRAV) bands appear and that above 1600 cm^{-1} where the electronic absorption of free charge carriers are found with a maximum around 5000 cm^{-1} . The FTIR spectra also give evidence about the inclusion of the counterion PF_6^- indicated by a very intense peak at 842 cm^{-1} . The results of this FTIR spectroelectrochemical study point to a high concentration of the positive charge carriers, but no information about their nature is available which is to be clarified by electron paramagnetic resonance UV–vis–NIR spectroelectrochemistry.

In Situ ESR/UV–vis–NIR Study of the Copolymer Films.

Figure 4 presents the results of the *in situ* ESR/UV–vis–NIR spectroelectrochemistry during the p-doping of a **copMeHeTh** film as a representative example for such a copolymeric material. The spectra were taken in a potential range starting from -0.353 V where no oxidation reaction occurs up to the switching potential (E_s) where the current plateau is observed during the forward voltammetric scan. The cyclic voltammetry has trigger markers along the curve (Figure 4A) which represent the potentials where the ESR spectra together with optical spectra are measured. The resultant time/potential ESR dependence in Figure 4 exhibits the successive formation of paramagnetic charge carriers during the p-doping of the copolymer. Initially, a small ESR signal is observed which corresponds to a small amount of spins in the copolymer formed in the electropolymerization process. Even after electrochemical reduction (dedoping) a part of the structure remains unchanged and keeps the ESR signal. This ESR signal is increased during the forward scan, reached a maximum, and transferred into a broad line. This point, where the polaron concentration reaches its maximum at 0.491 V, is very close to the anodic peak potential of 0.475 V. Both the current and the ESR signal then decrease up to the switching potential of 0.947 V. This decrease indicates that a fraction of polarons are transformed into diamagnetic species at higher doping levels. During the backward scan, the ESR signal increases again, reaching a maximum at a higher potential of 0.571 V. It does not reach its initial value. During the dedoping process the intensity of the ESR signal is higher than during the doping. The ESR signal of the polarons is fitted by a single Lorentzian line over a doping region between 0.14 and 0.722 V.

The series of UV–vis–NIR spectra in Figure 5A shows the successive formation of the redox states in more detail for the p-doping of **copMeHeTh**. Initially, two absorption bands are found at high and low energy, 850 and 1650 nm, respectively. Each of these two bands has an associated second transition at higher energy (shifted by approximately 40 and 160 nm, respectively) attributed to the electronic transitions of spinless structure. These two bands are more intense than the two polaronic bands at lower doping level, suggesting the formation of the second polaronic species, the spinless polaron pair. Its bands appear at moderate doping level at 0.370 V. In addition, above potentials of 0.5 V a single broad absorption band is formed at 1310 nm which increases up to the reverse potential. It is attributed to the formation of a bipolaron. Thus, in this potential range both the polaron pair and the bipolaron are coexistent and being in equilibrium with the polaron. This situation is special for conducting polymers and found for thiophene derivatives.

When compared to its parent polymers, the homopolymers, the behavior of the copolymer can be interpreted in its structure effects on the electronic properties. This comparison, presented in Figure 6, shows the differences in the potential-dependent

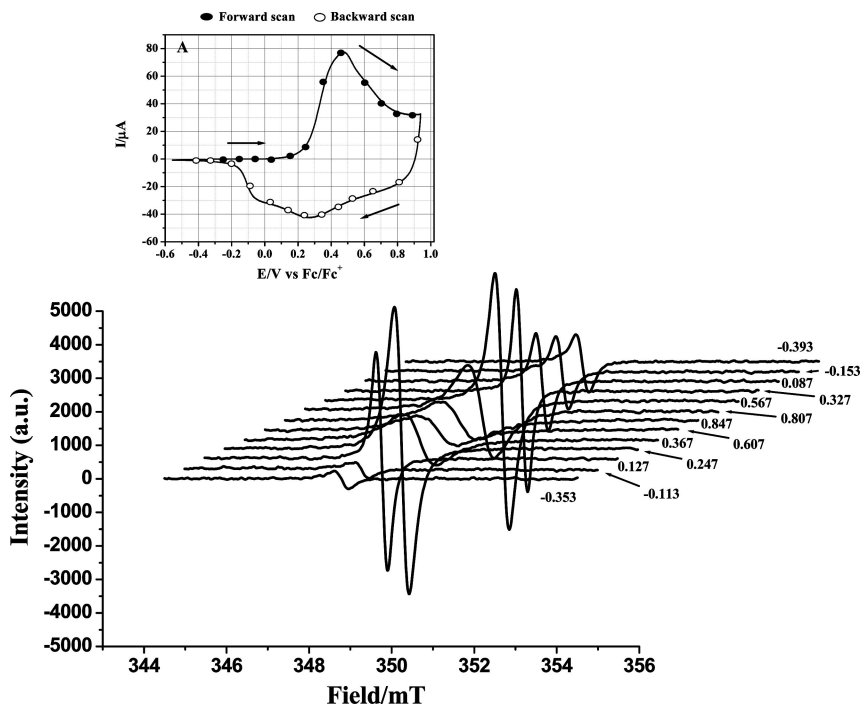


Figure 4. (A) Cyclic voltammetry of a **copMeHeTh** film on ITO electrode (ϕ 3 mm) in acetonitrile + 0.1 M *n*-Bu₄NPF₆ at a scan rate of 0.01 V s⁻¹. The circles along the voltammogram represent the triggers for the ESR and the UV–vis–NIR measurements. (Below) *In situ* simultaneously measured ESR spectra of **copMeHeTh** are given. Twenty-five spectra were recorded during one p-doping cycle of the copolymer.

behavior of the three types of polymer structures. Thus, the dedoping of the **copMeHeTh** is less difficult at early stages than for the **p-3-HeTh** film while the dedoping of **p-3-MeTh** is faster to result in lower polaron concentrations. In all the three conducting polymer films the doping is not completely reversible because the ESR signal has a higher intensity at the end of a voltammetric scan than in the initial state. In the **p-3-HeTh** film the ESR signal starts to increase strongly at the beginning of the reversed scan. Therefore, the **p-3-HeTh** stabilizes the polarons to a higher extent than the **copMeHeTh** film at the beginning of the dedoping, while in **p-3-MeTh** film the polaron is preferably formed during the doping process according to the high ESR intensity in the forward scan. Therefore, the alkyl substituent in the 3-position has a strong influence on the formation of the polarons being in addition dependent on the absence or presence of higher charged states.

A correlation of the current–potential dependence in the cyclic voltammogram (Figure 1) with the ESR signal–potential profile (Figure 6) gives a clear insight into the formation of the polaron in a certain polymer structure upon doping. As the ESR signal of the **p-3-HeTh** film starts to grow up at a potential value (0.118 V) between the **p-3-MeTh** film (0.008 V) and the **copMeHeTh** film (0.127 V), the energy of polaron formation in the copolymer is not the medium value of the monomers. The maximum of the polaron concentration in the p-doping of the **copMeHeTh** and **p-3-HeTh** is reached at similar potentials, 0.488 and 0.475 V, respectively, being consistent with the maximum of the anodic peak potential (Figure 1A) and the first broad anodic peak potential (Figure 1B), respectively. In contrast, the maximum amount of polarons for the **p-3-MeTh** is reached at lower energy (0.374 V).

The formation of polarons and subsequently of diamagnetic doubly charged species upon oxidation of the three films is evidenced from the potential profile of the relative intensity of the ESR signal (Figure 6). The evidence for the formation of the polarons (P⁺), polaron pairs (PP²⁺), and bipolarons (BP²⁺)

has been obtained by the UV–vis–NIR spectroscopy applied in parallel to ESR spectroscopy at the working electrode during cyclic voltammetry.²¹ The absorption spectra for the **copMeHeTh** film are shown in Figure 5A. At early stages of the doping the absorption bands at 850 and 1650 nm associated with polarons from **copMeHeTh** are located at the same wavelengths as the polaronic bands of **p-3-MeTh** while the polaronic bands of **p-3-HeTh** appear at 705 and 1689 nm. In all the three cases, upon oxidation the polaronic bands are blue-shifted and their relative intensity is increased while the intensity of the ESR signal as a measure for the polaron concentration is decreased. Therefore, this blue shift in absorption is attributed to the formation of the diamagnetic polaron pair with a similar absorption pattern as the polaron. Therefore, only the simultaneous use of both the ESR and the UV–vis–NIR spectroscopy enables the differentiation of polarons (paramagnetic) and polaron pairs (diamagnetic).

At high doping levels but different reverse potentials a new band appears (BP²⁺) in the middle of the two polaronic transitions at 1310 nm (**copMeHeTh**), 1380 nm (**p-3-HeTh**), and 1300 nm (**p-3-MeTh**) which is attributed to the bipolaron. The development of the optical absorption signal consisting of the three absorption peaks (polaron pair and bipolaron) results in a decrease of the ESR signal, indicating the transformation of the polarons into polaron pairs and bipolarons. The time/potential dependence of the ESR and the UV–vis–IR intensity of the polymers in these measurements are comparable to the results of a previous study of the doping of **p-3-MeTh**.^{22,23}

According to the cyclic voltammetry and the potential profiles of ESR intensities, the electrochemical oxidation of **copMeHeTh** and the formation of polarons in this copolymer occur at higher potentials than in **p-3-MeTh** and at lower potentials (for the second broad anodic peak) in **p-3-HeTh**. This is an indication of the lower density of the long alkyl side chains in the copolymer **copMeHeTh** due to the presence of the methyl groups which contribute to a reduction of the

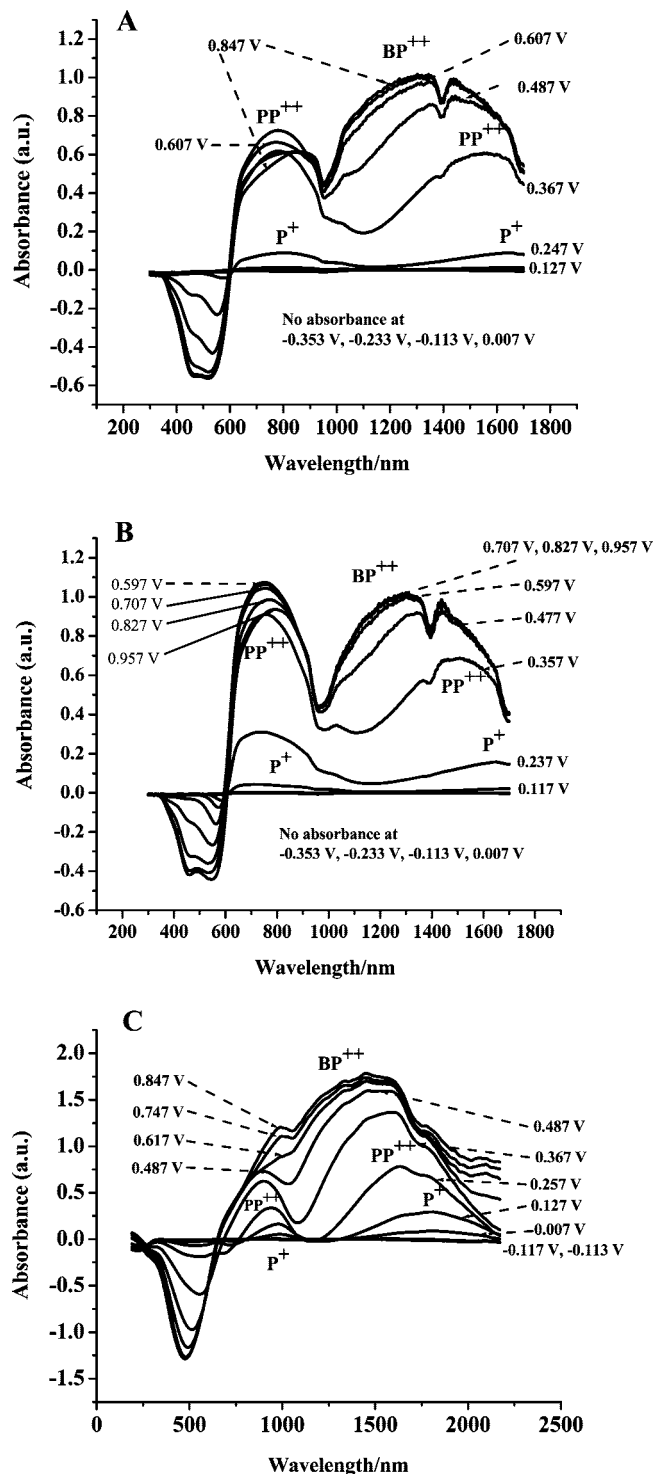


Figure 5. *In situ* simultaneously measured UV-vis-NIR spectra of **copMeHeTh** (A), **p-3-HeTh** (B) and **p-3MeTh** (C). Twenty-five (**copMeHeTh**), twenty-seven (**p-3-HeTh**) and twenty-three (**p-3MeTh**) spectra were recorded during one p-doping cycle.

side-chain interactions by separating the long side chains from each other. As a consequence, the low density may allow dopant anions to enter easily into the films in contrast with a substantially dense **p-3-HeTh** film in which the electrochemical oxidation requires a higher energy. In contrast, the **p-3-MeTh** film presents smaller side-chain interactions which favor the injection and rejection of the dopants during the doping and dedoping, respectively.

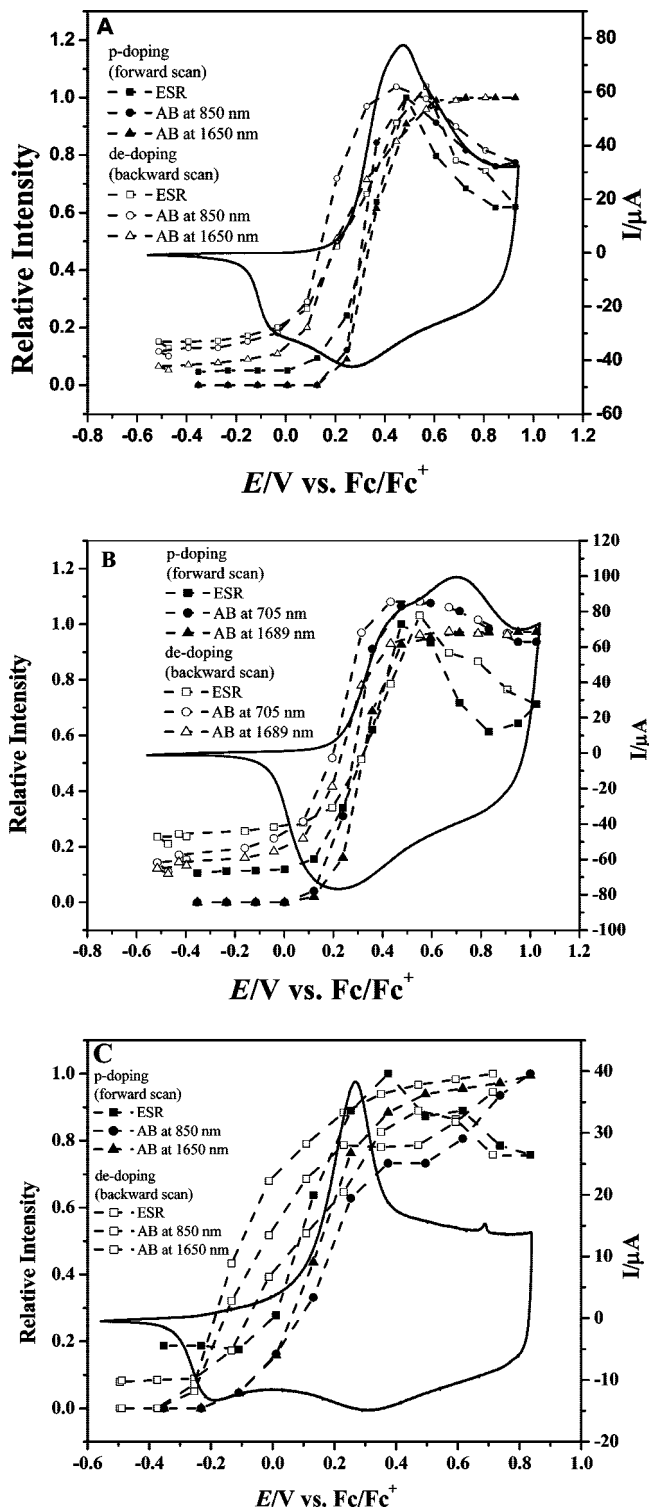


Figure 6. Potential dependence of the relative intensity of the ESR signal and the optical absorption bands (AB) in the UV-vis and NIR of **copMeHeTh** (A), **p-3HeTh** (B), and **p-3MeTh** (C) films at higher doping levels in a cyclic voltammetric scan.

The ESR and UV-vis-IR potential profiles of **p-3-MeTh** favor the formation of diamagnetic species at high doping levels which are predominately bipolarons. During the discharging the ESR signal is lower than during the doping process pointing to the low stability of polarons in this homopolymer. In literature data the predominant charge carriers in polythiophene and **p-3-MeTh** films at higher doping levels are expected to be bipolarons,^{24–27} which is consistent with our results.

Conclusions

A detailed spectroelectrochemical study of the p-doping of **copMeHeTh** and its homopolymers gives an insight into the structure of the copolymer and its changes upon doping. FTIR studies of the copolymer **copMeHeTh** points to its regioregular structure, as compared with the parent homopolymers **3-HeTh** and **3-MeTh** which seem to be more irregular. The *in situ* ESR/UV-vis-NIR spectroelectrochemistry gives a clear evidence for a formation of polarons while at higher doping both the polaron pairs and the bipolaron are formed in **3-HeTh** as well as the copolymer **copMeHeTh**. During the p-doping of **3-MeTh** bipolarons are the dominating species at higher doping levels. It is demonstrated that only the simultaneous use of both the ESR and the UV-vis-NIR spectroscopy enables the differentiation of polarons (paramagnetic) and polaron pairs (diamagnetic) in a conducting polymer.

Acknowledgment. This work was supported by Sonderforschungsbereich 287 (SFB 287) of the Deutsche Forschungsgemeinschaft (DFG) for L.F.C.R. and A.K. and a SMWK grant (A.K.), which is gratefully acknowledged. We thank Dr. I. Mönch and co-workers (IFW Dresden) for preparing the gold coatings on the ATR crystal.

References and Notes

- (1) Roncali, J. *Chem. Rev.* **1992**, 92, 711–738.
- (2) (a) Street, G. B.; Brédas, J. L. *Acc. Chem. Res.* **1985**, 18, 309–315. (b) Costanzo, F.; Tonelli, D.; Scalmani, G.; Cornil, J. *Polymer* **2006**, 47, 6692–6697.
- (3) Pei, Q.; Inganäs, O.; Gustafsson, G.; Granström, M.; Andersson, M.; Hjertberg, T.; Wennerström, O.; Österholm, J. E.; Laakso, J.; Järvinen, H. *Synth. Met.* **1993**, 55–57, 1221–1226.
- (4) Gustafsson, G.; Inganäs, O.; Nilsson, J. O.; Liedberg, B. *Synth. Met.* **1988**, 26, 297–309.
- (5) Hotta, S.; Soga, M.; Sonoda, N. *Synth. Met.* **1988**, 26, 267–279.
- (6) Hotta, S. *Synth. Met.* **1987**, 22, 103–113.
- (7) (a) Rapta, P.; Neudeck, A.; Petr, A.; Dunsch, L. *J. Chem. Soc., Faraday Trans.* **1998**, 94, 3625–3630. (b) Neudeck, A.; Petr, A.; Dunsch, L. *Synth. Met.* **1999**, 107, 143–158.
- (8) (a) Sturm, J.; Künzelmann, U.; Bischoff, S.; Dunsch, L. *Brüker-Report No. 142*, **1996**; pp 8–11. (b) Zimmermann, A.; Künzelmann, U.; Dunsch, L. *Synth. Met.* **1998**, 93, 17–25. (c) Zimmermann, A.; Dunsch, L. *J. Mol. Struct.* **1997**, 410–411, 165–171.
- (9) Chen, T. A.; Rieke, R. D. *J. Am. Chem. Soc.* **1995**, 117, 233–244.
- (10) Buzarovska, A.; Arsov, L.; Hebestreit, N.; Plieth, W. *J. Solid State Electrochem.* **2002**, 5, 49–54.
- (11) Singh, R.; Kumar, J.; Singh, R. K.; Kaur, A.; Sood, K. N.; Rastogi, R. C. *Polymer* **2005**, 46, 9126–9132.
- (12) Xu, B.; Holdcroft, S. *Macromolecules* **1993**, 26, 4457–4460.
- (13) Trznadel, M.; Pron, A.; Zagórska, M. *Synth. Met.* **1999**, 101, 118–119.
- (14) Jiang, X.; Patil, R.; Harima, Y.; Ohshita, J.; Kunai, A. *J. Phys. Chem. B* **2005**, 109, 221–229.
- (15) Jiang, X.; Harima, Y.; Yamashita, K.; Tada, Y.; Ohshita, J.; Kunai, A. *Chem. Phys. Lett.* **2002**, 364, 616–620.
- (16) Skompska, M.; Szkurlat, A. *Electrochim. Acta* **2001**, 46, 4007–4015.
- (17) Harima, Y.; Jiang, X.; Patil, R.; Komaguchi, K.; Mizota, H. *Electrochim. Acta* **2007**, 52, 8088–8095.
- (18) (a) Schaffer, H. E.; Heeger, A. J. *Solid State Commun.* **1986**, 59, 415–421. (b) Heeger, A. J.; Kivelson, S.; Schrieffer, J. R.; Su, W.-P. *Rev. Mod. Phys.* **1988**, 60, 781–850. (c) Christensen, P. A.; Hamnett, A.; Read, D. C. *Electrochim. Acta* **1994**, 39, 187–196.
- (19) (a) Neugebauer, H.; Nauer, G.; Neckel, A.; Tourillon, G.; Garnier, F.; Lang, P. *J. Phys. Chem.* **1984**, 88, 652–654. (b) Kim, Y. H.; Hotta, S.; Heeger, A. J. *Phys. Rev. B* **1987**, 36, 7486–7490. (c) Hernandez, V.; Ramirez, F. J.; Otero, T. F.; Lopez Navarrete, J. T. *J. Chem. Phys.* **1994**, 100, 114–129.
- (20) Hotta, S.; Soga, M.; Sonoda, N. *J. Phys. Chem.* **1989**, 93, 4994–4998.
- (21) van Haare, J. A. E. H.; Havinga, E. E.; van Dongen, J. L. J.; Janssen, J. L. R. A. J.; Cornil, J.; Brédas, J. L. *Chem.—Eur. J.* **1998**, 4, 1509–1522.
- (22) Tarábek, J.; Rapta, P.; Jähne, E.; Ferse, D.; Adler, H.-J.; Maumy, M.; Dunsch, L. *Electrochim. Acta* **2005**, 50, 1643–1651.
- (23) Rapta, P.; Lukkari, J.; Tarábek, J.; Salomäki, M.; Jussila, M.; Johannes, G.; Riekkola, M.-L.; Kankare, J.; Dunsch, L. *Phys. Chem. Chem. Phys.* **2004**, 6, 434–441.
- (24) Jiang, X.; Harima, Y.; Zhu, L.; Kunugi, Y.; Yamashita, K.; Sakamoto, M.; Sato, M. *J. Mater. Chem.* **2001**, 11, 3043–3048.
- (25) Harima, Y.; Kunugi, Y.; Yamashita, K.; Shiotani, M. *Chem. Phys. Lett.* **2000**, 317, 310–314.
- (26) Harima, Y.; Eguchi, T.; Yamashita, K. *Synth. Met.* **1998**, 95, 69–74.
- (27) Harima, Y.; Eguchi, T.; Yamashita, K.; Kojima, K.; Shiotani, M. *Synth. Met.* **1999**, 105, 121–128.

JP806810R